JOURNAL OF GEOPHYSICAL RESEARCH, VOL. 111, D23S23, doi:10.1029/2006JD007475, 2006

A wind profiler trajectory tool for air quality transport applications

Allen B. White,[1,2] Christoph J. Senff,[1,2] Ann N. Keane,[3] Lisa S. Darby,[3] Irina V. Djalalova,[1,2] Dominique C. Ruffieux,[1,4] David E. White,[1,2] Brent J. Williams,[5] and Allen H. Goldstein[5]

Received 3 May 2006; revised 13 September 2006; accepted 27 September 2006; published 12 December 2006.

[1] Horizontal transport is a key factor in air pollution meteorology. In several recent air quality field campaigns, networks of wind profiling Doppler radars have been deployed to help characterize this important phenomenon. This paper describes a Lagrangian particle trajectory tool developed to take advantage of the hourly wind observations provided by these special profiler networks. The tool uses only the observed wind profiles to calculate trajectory positions and does not involve any model physics or parameterizations. An interpolation scheme is used to determine the wind speed and direction at any given location and altitude along the trajectory. Only the horizontal winds measured by the profilers are included because the type of profiling radars used in this study are unable to resolve synoptic-scale vertical motions. The trajectory tool is applied to a case study from the International Consortium for Research on Transport and Transformation air quality experiment conducted during the summer of 2004 (ICARTT-04). During this international field study, air chemistry observations were collected at Chebogue Point, a coastal station in southwestern Nova Scotia, and factor analysis was used to identify time periods when air pollution from the United States arrived at the site. The profiler trajectories are compared to trajectories produced from numerical model initialization fields. The profiler-based trajectories more accurately reflect changes in the synoptic weather pattern that occurred between operational upper air soundings, thereby providing a more accurate depiction of the horizontal transport responsible for air pollution arriving in Nova Scotia.

Citation: White, A. B., C. J. Senff, A. N. Keane, L. S. Darby, I. V. Djalalova, D. C. Ruffieux, D. E. White, B. J. Williams, and A. H. Goldstein (2006), A wind profiler trajectory tool for air quality transport applications, *J. Geophys. Res.*, *111*, D23S23, doi:10.1029/2006JD007475.

1. Introduction

[2] Lagrangian-based particle trajectory models are useful for studying the transport of atmospheric constituents such as aerosols, ozone, and water vapor. Several model-based trajectory tools already exist. The HYbrid Single-Particle Lagrangian Integrated Trajectory (HYSPLIT) model developed by the NOAA Air Resources Laboratory (http://www.arl.noaa.gov/ready/hysplit4.html) and the FLEXPART model developed by the Norwegian Institute of Air Research (http://zardoz.nilu.no/~andreas/flextra+flexpart.html) are two commonly used approaches.

[3] The NOAA Earth System Research Laboratory (NOAA/ESRL) has developed an observationally based trajectory tool that uses data from wind profiler networks to calculate forward or backward particle trajectories. The tool is purely observationally based, i.e., there are no model physics or parameterizations involved. The trajectory algorithm applies an inverse distance squared weighting function to the observations from profiler networks in order to determine the hourly position of the trajectories.

[4] The profiler trajectory tool was first developed for the Southern Oxidants Studies (SOS) [*Meagher et al.*, 1998]. Two of the SOS field experiments occurred in and around Nashville, Tennessee, during the summers of 1995 and 1999. For each study, profiler networks were installed to measure transport in and out of the urban area. *McNider et al.* [1998] performed spectral decomposition on a time series of zonal and meridional wind components measured by one of the 1995 field study profilers located in rural farmland approximately 55 km west of Nashville. Two primary peaks in spectral density appeared in the power spectra (Figure 1). The first spectral peak was more prominent at higher altitudes and had a period of approximately 5 days. This peak was associated with variations in synoptic-scale weather. A second spectral peak was more prominent at lower altitudes and had a period of approximately 20 hours. This peak was associated with the inertial oscillation. The

[1]Cooperative Institute for Research in Environmental Sciences, University of Colorado, Boulder, Colorado, USA.
[2]Also at Earth System Research Laboratory, NOAA, Boulder, Colorado, USA.
[3]Earth System Research Laboratory, NOAA, Boulder, Colorado, USA.
[4]Now at Aerological Station, MeteoSwiss, Payerne, Switzerland.
[5]Department of Environmental Science, Policy, and Management, University of California, Berkeley, California, USA.

0148-0227/06/2006JD007475$09.00

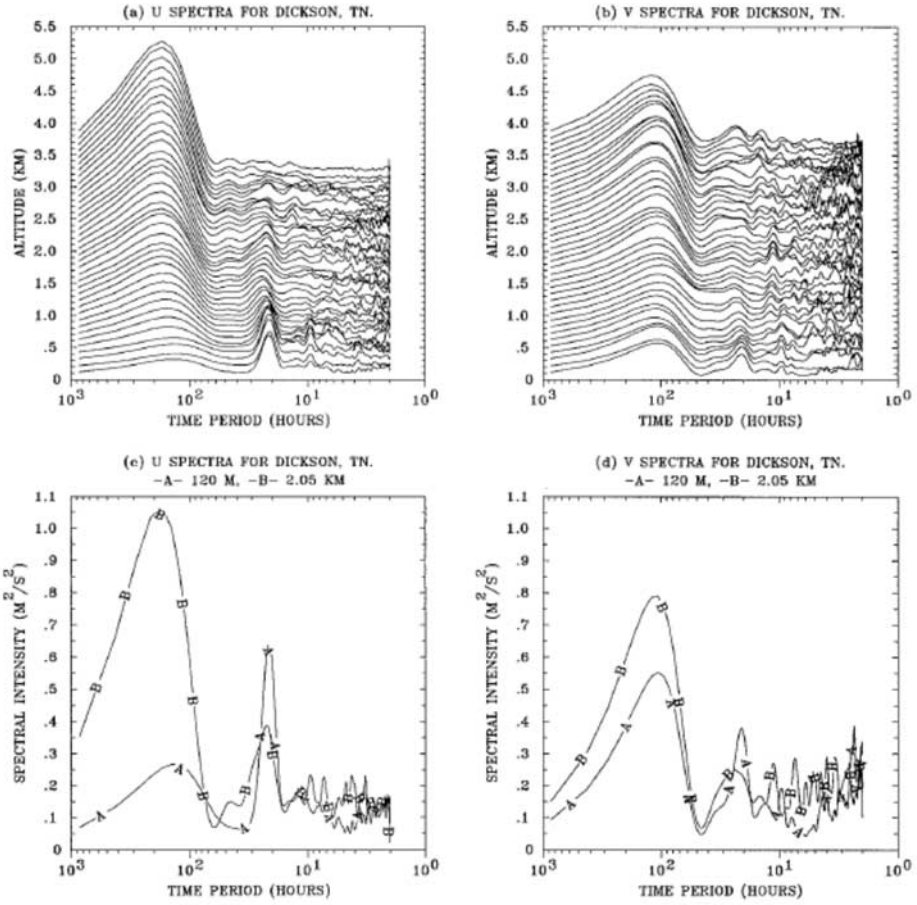

Figure 1. Horizontal wind energy spectra computed from wind profile observations taken by the 915-MHz wind profiler located at Dickson, Tennessee, during the 1995 Southern Oxidants Study. Zonal and meridional wind component spectra are plotted (a and b) as a function of altitude and (c and d) for selected altitudes of 120 m (labeled "A") and 2.05 km (labeled "B"). After *McNider et al.* [1998].

inertial period is given by $2\pi/f$, where f is the Coriolis parameter. For the profiler site used in this analysis, $f = 8.624 \times 10^{-5}\ s^{-1}$. The theoretical inertial period is then 20.2 hours, which agrees well with the period of the observed spectral peak in the zonal and meridional wind component power spectra produced from the wind profiler data.

[5] Under weak synoptic forcing, a nocturnal low-level jet was often observed in the wind profiles collected by the profiler networks deployed for the SOS field experiments. The vertical shear associated with the jet, along with the rotation caused by the inertial force, which were both experienced at night because the flow above the shallow nocturnal inversion is decoupled from the effects of surface friction, would hypothetically cause horizontal transport to vary significantly with altitude. NOAA scientists believed they could document and quantify this behavior using Lagrangian trajectories calculated from the wind profiles measured by the profiler network. This was the primary motivation for developing the profiler trajectory tool. An example from the 1995 Nashville field study that demonstrates the influences of the inertial oscillation and the low-level jet on nocturnal regional transport is shown in Figure 2. The trajectories for the two lowest altitude ranges cover the largest distance, indicating the presence of stronger winds at these altitudes. The trajectory for the highest altitude range is furthest removed from the low-level jet and the influence of surface friction. It is here that the rotation caused by the inertial force is most evident. The method used to derive these trajectories is described in section 3.

[6] The profiler-based trajectories have been used in studies related to SOS [*Banta et al.*, 1998], for the 2000 Texas Air Quality Study [*Banta et al.*, 2005], and more recently for the 2002 New England Air Quality Study (L. S. Darby et al., manuscript in preparation, 2006) and the 2004 International Consortium for Atmospheric Research on Transport and Transformation field study (ICARTT-04) that focused on outflow of air pollution from North America [*Fisher et al.*, 2006; *Millet et al.*, 2006; *White et al.*, 2006; B. J. Williams et al., Chemical speciation of organic aerosol during ICARTT 2004: Results from in situ measurements, submitted to *Journal of Geophysical Research*, 2006, hereinafter referred to as Williams et al., submitted manuscript, 2006]. For the first time, the profiler trajectory tool is available on the Internet in real time for the 2005–2006

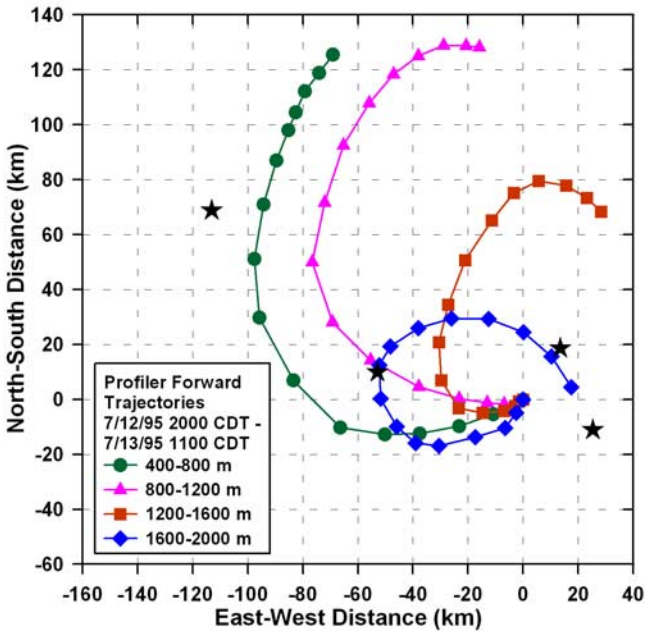

Figure 2. Forward trajectories for the dates, times, and altitudes shown at the bottom left. The trajectories are calculated from wind profiler observations collected during the 1995 Southern Oxidants Study Nashville/Middle Tennessee intensive. The locations of the wind profilers are indicated by the stars. These overnight trajectories demonstrate the combined effects of a nocturnal low-level jet and the inertial oscillation on regional transport.

Texas air quality study (TEXAQS-II). In section 4 we apply the profiler-based trajectory method to a case study from ICARTT-04.

2. Wind Profilers

[7] Wind profilers are Doppler radars that operate most often in the UHF or VHF frequency bands. Four primary types of wind profilers were in operation in the United States at the time of this publication. The NOAA Profiler Network (NPN) profilers are fixed radars that operate at a frequency of 404 MHz [*Chadwick*, 1988], although a frequency conversion to 449 MHz has been mandated by the Federal Communications Commission. A smaller, transportable, wind profiler used by NOAA research and other agencies is the 915-MHz boundary layer wind profiler [*Carter et al.*, 1995]. The NPN profilers provide the deepest coverage of the atmosphere, but lack coverage in the planetary boundary layer (PBL). The 915-MHz profilers provide the best coverage of winds in the PBL, but they lack height coverage much above the PBL. A third type of wind profiler that operates at 449 MHz (the so-called¼-scale 449-MHz profiler) combines the best sampling attributes of the other two systems. The U.S. Air Force has recently installed several of these radars along the southern U.S. border. The 50-MHz wind profiler is the oldest type of radar wind profiler produced in the United States [*Ecklund et al.*, 1979]. It is useful for deep atmospheric probing, but provides very little information in the boundary layer [*Frisch et al.*, 1986].

[8] Wind profilers transmit pulses of electromagnetic radiation vertically and in at least two slightly off-vertical ($\sim$75° elevation) directions in order to resolve the three-dimensional vector wind. A small amount of the energy transmitted in each direction is reflected or backscattered to the radar antenna. The backscatter returns are Doppler shifted by the motion of the scattering media. Profilers receive backscatter returns from atmospheric features (turbulence, clouds, precipitation) and nonatmospheric features (insects, birds, trees, airplanes, radio-frequency interference). The challenge in signal processing is to avoid the returns from nonatmospheric scattering targets and focus on the atmospheric returns. To do this, profilers sample thousands of consecutive transmitted pulses to boost the signal-to-noise ratio of the atmospheric returns, a process known as "coherent integration."

[9] The return signals are sampled at discrete intervals called range gates. The size of the range gates is determined by the length of the transmitted pulse, which is usually on the order of hundreds to thousands of nanoseconds (ns). For example, a 700-ns pulse translates into a true range resolution (i.e., one without oversampling) of 105 m. Once the range-gated Doppler shifts from a set of beams have been determined, a wind profile is calculated. This process usually occurs over an observing period of 30 to 90 s. The wind profiles measured within a specified averaging period (15 min to 60 min) are averaged together using a consensus routine. The consensus routine filters outliers using threshold and acceptance windows. The consensus wind profiles are archived on site and transmitted back to a data hub in Boulder, Colorado, via phone lines or, in remote areas, via satellite communications. Postprocessing data quality control is applied using the continuity method developed by *Weber et al.* [1993]. The accuracy of horizontal winds measured by the profiler is better than 1 m s^{-1} on the basis of comparison with balloon soundings [*Martner et al.*, 1993]. The accuracy of profiler vertical-velocity measurements is less certain [e.g., *Worthington*, 2002].

3. Wind Profiler Trajectory Tool

[10] The wind profiler data arriving from field sites are converted to a common format and placed in a database for use by the trajectory tool. The tool can be used in post-experiment analysis activities, and beginning with the TEXAQS-II study in 2005 (http://esrl.noaa.gov/csd/2006/), in near real time to support mission planning activities and NWS forecast operations (see http://www.etl.noaa.gov/programs/2006/texaqs/traj/). The user has the option of calculating forward or backward trajectories and specifying the start/end point location and the period over which to calculate the trajectories. Other options include specifying multiple altitude ranges and the number of profilers to use or exclude in the calculations. For locations over water, the user may request surface trajectories that are produced from available buoy and shoreline surface wind observations and upper air trajectories that include wind profile observations from the NOAA Research Vessel *Ronald H. Brown*, when available (see Figure 3 or http://www.etl.noaa.gov/programs/2004/neaqs/traj/).

[11] The profiler trajectory tool uses only the horizontal winds measured by the profilers. Wind profilers are not

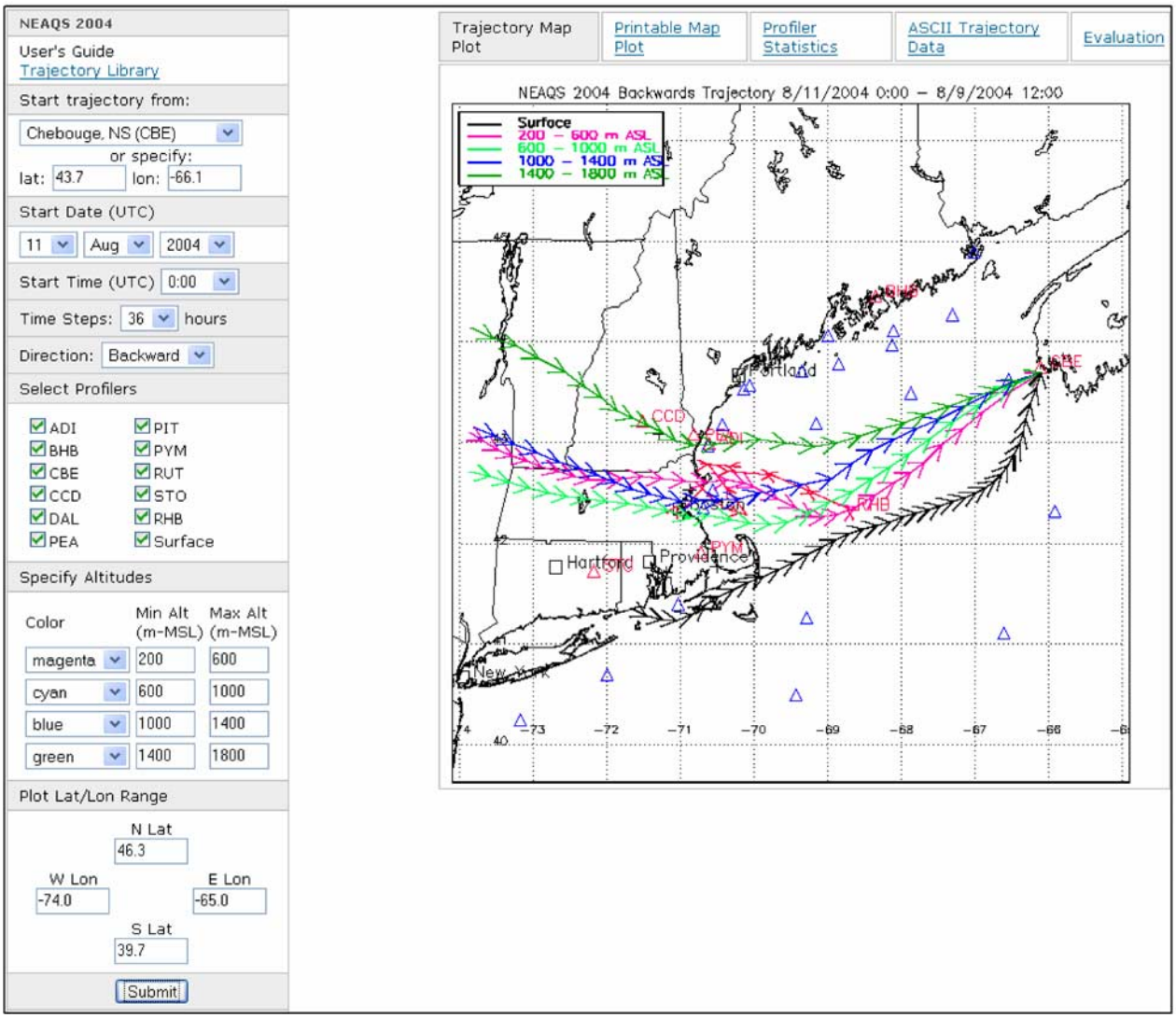

Figure 3. NOAA/ESRL wind profiler trajectory tool Internet interface. (left) User sets input parameters. (right) Trajectory output is displayed on the map. Arrowheads denote the position along each trajectory at hourly intervals. The red line shows the track of the NOAA Research Vessel *Ronald H. Brown* during the requested period. The locations of the profilers in the display domain are indicated by red triangles. The locations of buoy and shoreline observing stations are indicated by blue triangles. These maritime data sets were provided by NOAA's National Data Buoy Center, the Gulf of Maine Ocean Observing System, and the University of Maine.

capable of resolving synoptic-scale vertical motions measured on an hourly timescale, for example. In addition, a downward bias in the hourly averaged vertical-velocity measurements made within the convective boundary layer by the 915-MHz profilers has been identified [*Angevine*, 1997]. Because we neglect vertical motion, the profiler trajectories do not adhere to mass balance considerations and, therefore, may differ substantially from trajectories based on full three-dimensional simulations provided by numerical models. However, the increased time resolution of the wind profiler observations (hourly versus twice daily for the operational sounding network) and continuity of the profiler data, especially during active weather patterns, provide a more important benefit for the trajectory calculations. In the future, the most accurate trajectories may be produced by properly assimilating wind profiler data into a mesoscale model. The profiler trajectories are also only reliable within regions where the profiler networks exist. This limits their general application compared to model-based trajectories and, more specifically, limits the spatial and temporal domains of the trajectories that can be produced by this method. The Internet versions of the trajectory tool allow users to specify maximum trajectory durations of 36 hours for the New England trajectory tool and 48 hours for the Texas trajectory tool. A longer trajectory period was allowed for the Texas trajectory tool because the area of interest was larger and there was a larger and more comprehensive network of profilers available for the Texas study. Users of either trajectory tool must use caution in interpreting the results, especially if the

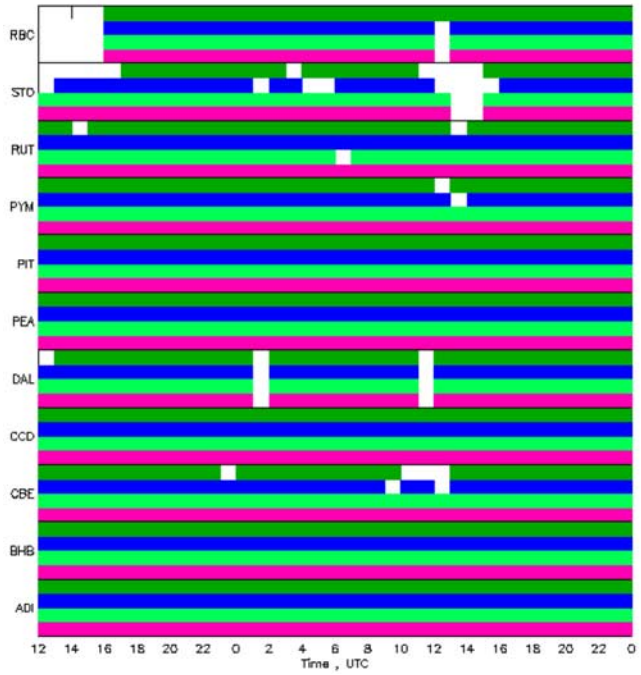

Figure 4. Sample profiler statistics output from the NOAA/ESRL trajectory tool. The *x* axis displays the time along the trajectory in hours. The *y* axis displays the three letter identifiers for the profilers selected in Figure 2. RBC refers to a combined data set that merges data from the *Ronald H. Brown* ship-based wind profiler and the ship-based Doppler lidar. The colored bars correspond to when profiler data were available for the trajectory analysis. Each color corresponds to one of the altitude ranges specified in Figure 3. White space appears when data from a particular profiler at a particular altitude range were not available.

trajectories pass outside the domain of the profiler network, where they become increasingly unreliable as the distance between the trajectory and the closest profiler observing site increases.

[12] For each hour in the requested trajectory period, the profiler trajectory algorithm uses all user-selected profilers in the network. The user has the option of deselecting one or more of the profilers, for example, if it is known that a profiler is malfunctioning, or to test the impact of a particular profiler or a set of profilers on the trajectory algorithm output. The algorithm computes the distance from the trajectory start point to all requested profiler locations, calculates the average wind speed and direction using an inverse distance squared weighting function, and calculates the trajectory for the first hour. If the trajectory starts or ends above a profiler location, or if the trajectory passes directly over a profiler site, a minimum distance of 0.01 km is assigned in order to avoid dividing by zero. Then this process is repeated for the remaining hours of the trajectory period using the trajectory end point of the previous hour as the reference point for the distance calculation. The weighting function technique is similar to creating a new set of gridded profiler winds for each hour in the trajectory period. Creating a full grid is not necessary because we are only interested in the one grid point that lies along the trajectory.

[13] If data from one of the requested profilers are not available at any given hour during the trajectory period, the weighted average will be computed from the remaining profilers. If the same profiler provides useable data at a later point in time during the trajectory period, it is again included in the average. If all selected profilers have a data outage at the same time, then the trajectory calculation is stopped at the hourly time step preceding the outage. No interpolation across data gaps is performed. Therefore a 1-hour data gap in all selected profilers truncates the trajectory.

[14] Profiler data measured at altitudes above mean sea level (msl) that fall into each of the user-specified altitude bins are averaged together. A future version of the profiler trajectory tool will allow users to choose the vertical frame of reference for the profiler data; either above msl or above ground level (agl). The agl frame of reference would be more appropriate to use, for example, when calculating low-level trajectories over complex terrain.

[15] Once the trajectory output has been plotted, the user has the option of getting a printable version of the trajectory map, creating a graphical representation of which profilers were included along each trajectory (Figure 4), retrieving ASCII text of the trajectory output, and filling out an evaluation form to let NOAA scientists and web developers know if the tool has been useful and/or to provide suggestions for how to improve the tool.

4. Case Study

[16] To demonstrate the value of incorporating hourly resolution winds in a trajectory analysis, we present a case study from ICARTT-04 [*Fehsenfeld et al.*, 2006]. The NOAA and cooperative agency wind profiler network available for this study is shown in Figure 5 and listed in Table 1. Operation of the shipboard wind profiler on the NOAA Research Vessel *Ronald H. Brown* was hindered by sea clutter (reflections from the ocean surface), which often prevented wind retrievals from this platform in the lowest 500 m above the surface. During ICARTT-04, scientists from NOAA/ESRL also deployed a high-resolution Doppler lidar (HRDL) onboard the Ronald H. Brown. HRDL provided high vertical resolution (up to 5 m) wind profiles in clear-sky conditions and/or below cloud base via the velocity-azimuth display (VAD) technique [*Browning and Wexler*, 1968]. After the field study, the wind profiles observed by HRDL were merged with the wind profiles observed by the wind profiler to improve altitude coverage, especially for the altitudes impacted by the sea clutter [*Wolfe et al.*, 2006].

[17] During ICARTT-04, scientists from the University of California at Berkeley measured speciated organics in aerosols with hourly time resolution using their Thermal Desorption Aerosol GC/MS-FID (TAG) instrument (Williams et al., submitted manuscript, 2006) at the Chebogue Point, Nova Scotia, observing station. The goal of these measurements was to define hourly changes in concentration for specific marker compounds that could be used to characterize the source of the aerosol. A factor analysis was carried out on the aerosol time series, including total organic mass and sulfate mass measured by the Aerodyne Research, Inc. Aerosol Mass Spectrometer (AMS), to

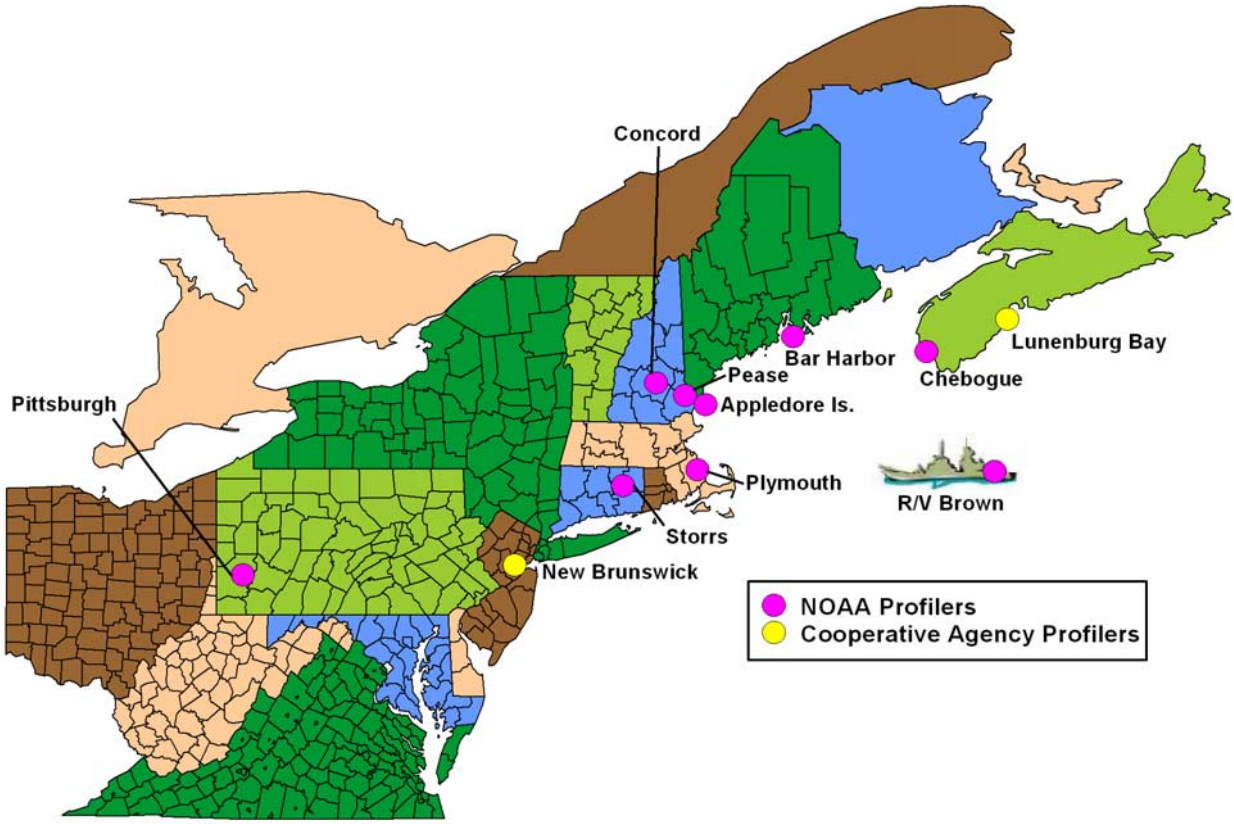

Figure 5. Map showing the locations of NOAA and cooperative agency observing sites in the ICARTT wind profiler network.

determine the relative contributions from different source categories or regions that were contributing to the total aerosol loading at each measurement time point [*Millet et al.*, 2006; Williams et al., submitted manuscript, 2006]. The influence of each factor at a particular time is determined by its score. The scores are constructed to have a mean of zero and a standard deviation of one. ''Impact periods'' for each factor are defined when the factor score exceeds one. One of the two factors attributed to pollution sources in the United States consisted of a high concentration of organic aerosol and sulfate, indicating a contribution from coal-fired power plant plumes. The score for this U.S. outflow factor peaked during a mid-August pollution episode (Figure 6).

[18] A synoptic weather map for this case is shown in Figure 7. At 1200 UTC on 9 August, a trough axis was located to the west of Nova Scotia and was followed further to the west by a ridge axis associated with high pressure centered over the mid-Atlantic U.S. coastline. The wind profiler data from Chebogue Point, Nova Scotia (CBE), are shown in Figure 8. Changes in wind direction in the lower troposphere that occurred with the passing synoptic features are clearly indicated early in the profiler data. The passage

Table 1. Locations of NOAA and Cooperative Agency Boundary Layer (915-MHz) Wind Profilers Available for the ICARTT Study

Location	Site Designator	Latitude, deg	Longitude, deg	Station Elevation, m	Sponsor
Appledore Island, Maine	ADI	42.99	−70.62	5	NOAA
Bar Harbor, Maine	BHB	44.44	−68.36	4	NOAA
Chebogue Point, Nova Scotia	CBE	43.70	−66.10	15	NOAA
Concord, New Hampshire	CCD	43.21	−71.52	104	NOAA
Lunenburg Bay, Nova Scotia	DAL	44.40	−64.30	30	Environment Canada
New Brunswick, New Jersey	RUT	40.50	−74.45	10	Rutgers University and the New Jersey Department of Environmental Protection
Pease International Tradeport, New Hampshire	PEA	43.09	−70.83	30	NOAA
Pittsburgh, Pennsylvania	PIT	40.48	−80.26	335	NOAA
Plymouth, Massachusetts	PYM	41.91	−70.73	46	NOAA
Research Vessel *Ronald H. Brown*	RHB	variable	variable	5	NOAA
Storrs, Connecticut	STO	41.80	−72.23	198	NOAA

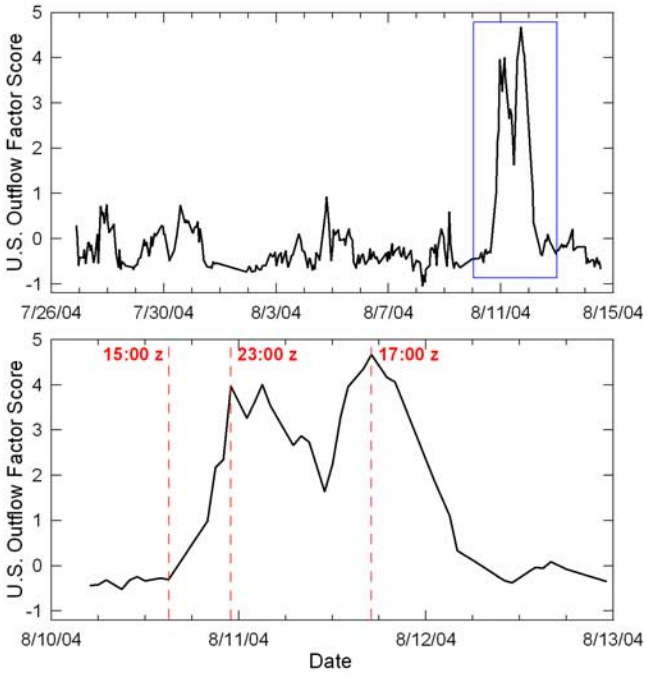

Figure 6. Time series of factor analysis score for U.S. outflow described by Williams et al. (submitted manuscript, 2006) (top) for the ICARTT field study and (bottom) for the period 10–12 August 2004. The U.S. outflow factor includes organic aerosol and sulfate. The vertical dashed lines indicate end times for back trajectory calculations shown in Figures 9, 10, and 13.

of the trough axis at approximately 0300 UTC on 10 August is indicated by a change from westerly to northwesterly flow near the surface. The subsequent passage of the ridge axis is indicated by the shift from northwesterly to weak westerly flow at 1500 UTC, which changes rapidly to southwesterly flow by 1800 UTC. Because the primary source of operational, upper air wind data in NOAA's observing system is the rawinsonde network, trajectory models that are based on numerical model initialization fields have access to updated upper air observations only every 12 hours, corresponding to the frequency of rawinsonde launches. Key changes in the synoptic conditions affecting the lower-tropospheric winds observed in this case evolved between soundings, which caused important discrepancies in the trajectories produced by the two methods.

[19] Figure 9 compares back trajectories computed using the wind profiler trajectory tool and the HYSPLIT model ending at 1500 UTC on 10 August. For this comparison and the comparisons that follow, the HYSPLIT model was run in its isobaric mode to allow for a more direct comparison with the constant altitude wind profiler trajectories. The input data for the HYSPLIT model were the 40-km-resolution gridded data from the Eta Data Assimilation System (EDAS). The discrete altitudes of the three HYSPLIT trajectories match roughly the middle of the altitude ranges used for three of the profiler-based trajectories. The two methods agree remarkably well at this time, only 3 hours after the EDAS wind field had been updated with rawinsonde data. At 1500 UTC, the air quality at the aerosol sampling site was good, as indicated by the low score of the U.S. outflow factor (Figure 6). Eight hours later, after the synoptic pattern had changed significantly, the agreement between the two trajectory methods was not as good (Figure 10).

[20] To investigate why the results from the two trajectory methods differed over the Gulf of Maine, we assembled wind profiles from the gridded 40-km EDAS using the NOAA/ARL's windgram display tool (http://www.arl.noaa.gov/ready.html) and compared them to the spatially interpolated wind profiles used in the profiler trajectory tool (i.e., using the method described in section 3). The results are shown in Figure 11 for two locations: Chebogue Point, Nova Scotia, the end point of the trajectories, and the Gulf of Maine (43°N and 68°W), where the difference between the results of the two trajectory methods is most obvious. At Chebogue Point (Figure 11a), the agreement between wind profiles from the wind profiler network and EDAS is fairly good. This explains why the HYSPLIT and wind profiler back trajectories do not diverge initially. The HYSPLIT trajectories are over the Gulf of Maine for approximately 17 hours, going back to 0600 UTC. However, most of the divergence between the two methods occurs between 1200 UTC and 1800 UTC, when the HYSPLIT trajectories make a decided turn to the northwest (Figure 10). The reason for this turn becomes evident by comparing the EDAS wind profiles over the Gulf of Maine at 1200 UTC and 1500 UTC (Figure 11b). There is a marked shift in wind direction that is most pronounced at the lowest levels, which is consistent with the sharpness of the bend in the lowest HYSPLIT trajectory. Because the profiler network winds turn to a more westerly direction by 0900 UTC and transition gradually to southerly component flow over the next 6 hours, it appears the EDAS interpolation scheme overestimated the period when the winds over the Gulf of Maine were influenced by the trough. Over land (i.e., before 0600 UTC on 10 August) the two trajectory methods are in better agreement (roughly parallel) because both the EDAS and profiler network winds were more uniformly from the

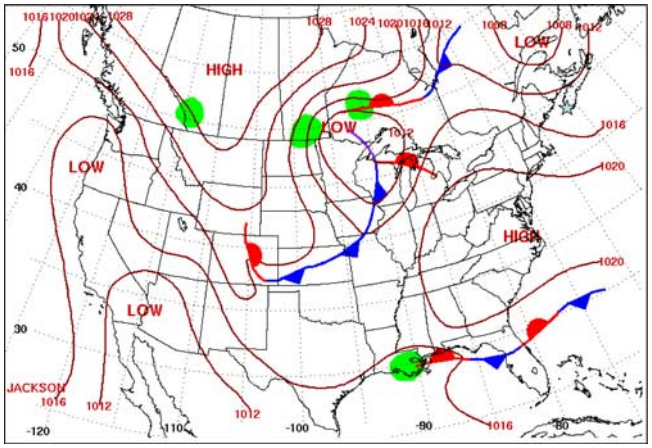

Figure 7. Surface weather map for 1200 UTC on 9 August 2004. The Chebogue Point, Nova Scotia, observing site (CBE) is indicated by the blue star. Map courtesy of NOAA's Hydrometeorological Prediction Center.

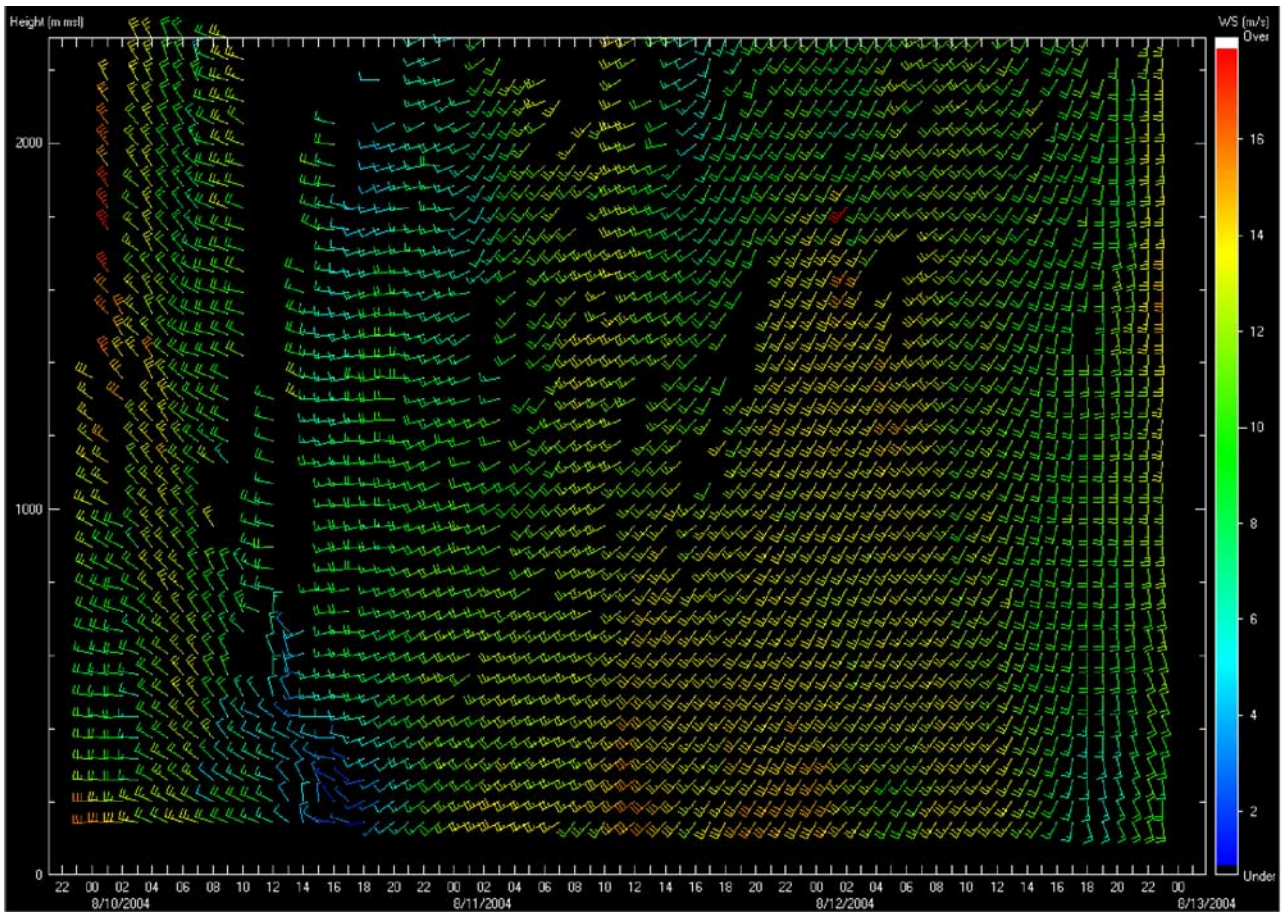

Figure 8. Time series of wind profiler data from Chebogue Point, Nova Scotia (CBE), for the period indicated along the bottom axis. The vertical axes indicate altitude in m above mean sea level (msl). Each full barb represents a wind speed increment of 5 m s^{-1}. Wind speed is also color coded to the vertical scale on the right. Gaps in data coverage are caused by removal of erroneous winds in postprocessing quality control or by undetectable atmospheric signal.

west-northwest, demonstrating the actual position and period of influence of the trough passage.

[21] The reason for the significant vertical motion in the HYSPLIT trajectories evident prior to 0600 UTC in Figure 10 is not certain, however the sinking motion indicated from about 0000 UTC to 0600 UTC is consistent with downslope flow on the east side of the Appalachian Mountains in northern New Hampshire and western Maine. In addition, the synoptic-scale vertical motion diagnosed by the pressure vertical velocity (ω) calculated from the EDAS fields (not shown) indicated persistent downward motion throughout the lower to mid troposphere (surface to 500 mbar) over Maine during this period.

[22] Transport of U.S. air pollution increased by 2300 UTC, as indicated by the local peak in the U.S. outflow factor score (Figure 6). It is unlikely that the pollution plume with high sulfate content sampled at Chebogue Point, Nova Scotia, originated in northern New England and passed over western Maine, as indicated by the HYSPLIT trajectories, because there are only a few small coal-fired power plants located there. It is more likely that the pollution originated further south, as indicated by the profiler-based trajectories, where a higher concentration of large coal-fired power plants exists (see Figure 12).

[23] The southwesterly winds favorable for transporting U.S. outflow to Nova Scotia persisted on 11 August (Figure 8). Consequently, the factor score for U.S. outflow peaked at 1700 UTC on this day (Figure 6). Figure 13 compares wind profiler and HYSPLIT model trajectories at this time. Again, there is good agreement between the two methods, especially given that there is southwesterly flow throughout the region, and wind data from the 11 August 0000 UTC and 1200 UTC operational upper air soundings should have impacted the EDAS wind fields used by the HYSPLIT model.

5. Summary and Discussion

[24] Particle trajectory models are useful for investigating atmospheric pollutant transport. However, as demonstrated by the case study presented, the winds in the lower troposphere that transport pollutants regionally are not measured with sufficient temporal resolution to capture important changes associated with mesoscale and synoptic weather. NOAA/ESRL has developed a wind profiler trajectory tool that is purely observationally based. The Internet-based application can be used in postanalysis mode for the New England Air Quality Studies in 2002 and 2004 and

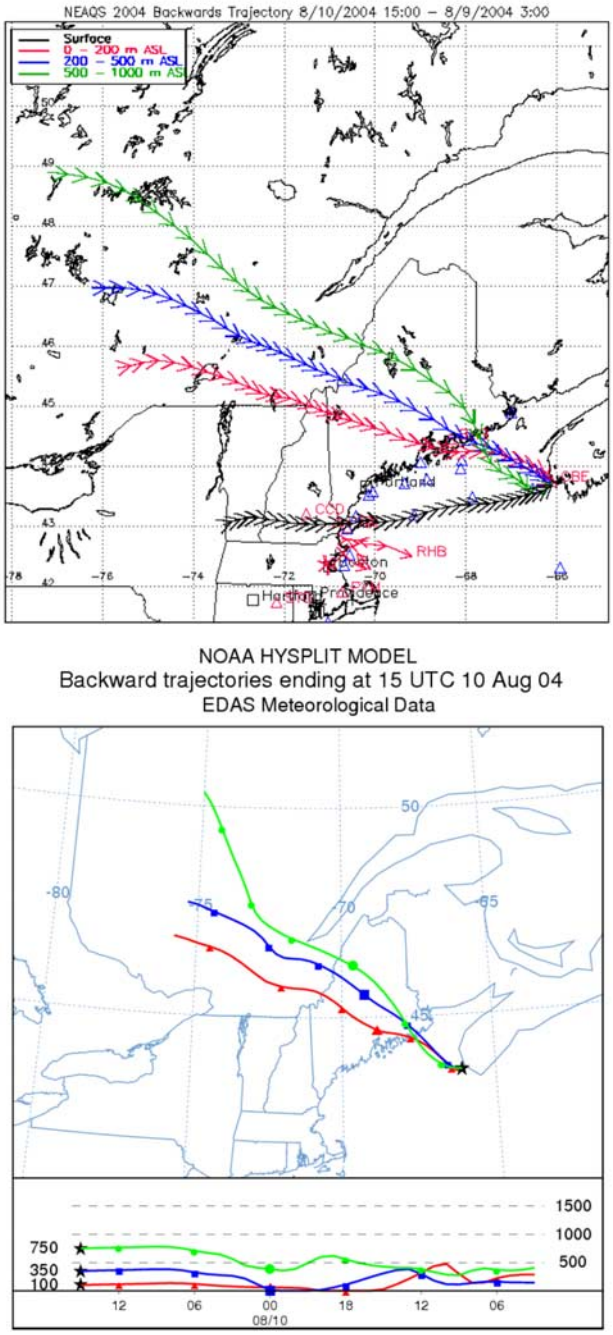

Figure 9. The 36-hour back trajectories ending at 1500 UTC on 10 August 2004, calculated from (top) wind profilers and (bottom) the HYSPLIT model. Profiler locations are marked by red triangles and red labels. Buoy and coastal surface observing stations are marked by blue triangles. The red line next to the RHB label plots the track of the NOAA Research Vessel *Ronald H. Brown* during the requested trajectory period. The surface trajectory (black curve) is calculated only from the buoy and coastal station data. The other trajectories in Figure 9 (top) are calculated from the land-based wind profiler network observations and the merged lidar/wind profiler data set from the *Ronald H. Brown*. The altitude of each HYSPLIT trajectory is at the center of the altitude range of the profiler trajectory with the matching color (red, blue, or green).

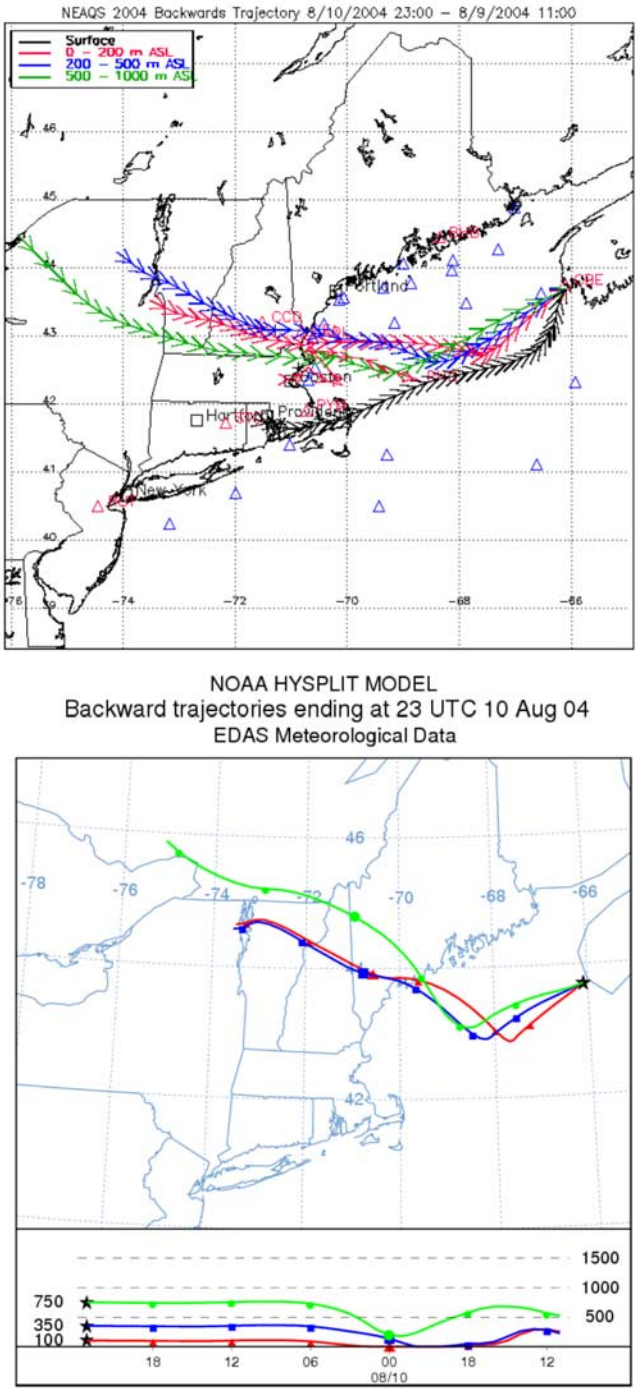

Figure 10. As in Figure 9 except ending at 2300 UTC on 10 August.

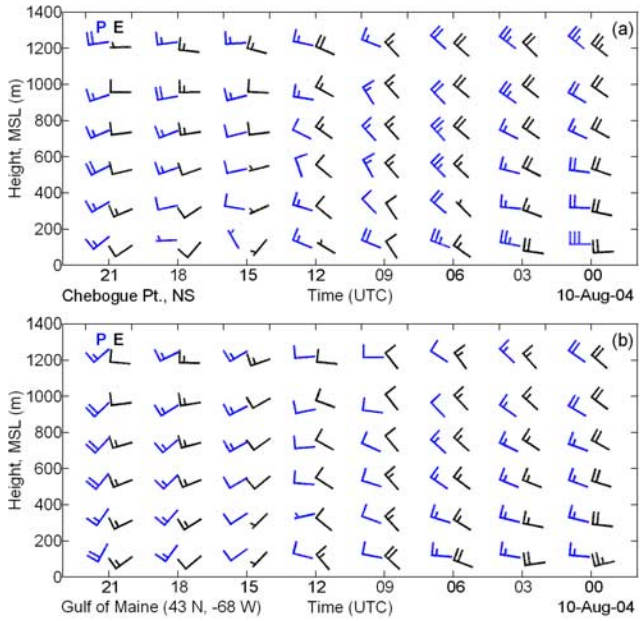

Figure 11. Comparison of wind profiles produced by the 40-km EDAS (E) and wind profiler network (P) from (a) Chebogue Point, Nova Scotia, and (b) the Gulf of Maine at 43°N and 68°W. Each full barb represents a wind speed increment of 5.0 m s^{-1}. The wind profiles from the profiler network were derived by combining the winds from the individual profiler sites using an inverse distance-squared weighting function (see text). The EDAS fields were converted from a pressure vertical coordinate to an altitude vertical coordinate using the 1976 Standard Atmosphere.

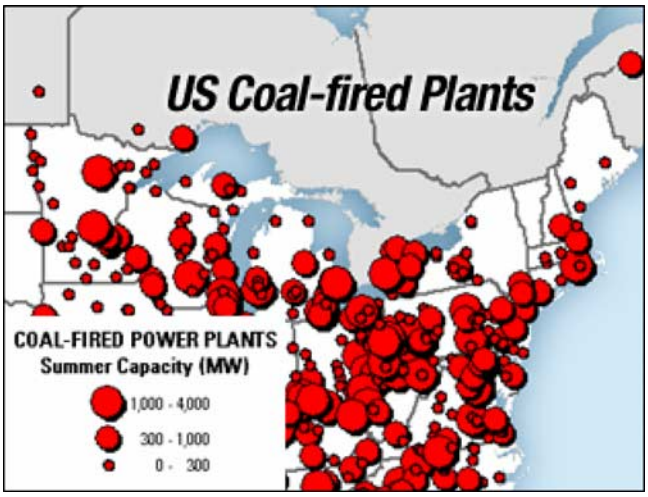

Figure 12. Distribution of coal-fired power plants in the northeastern United States as of 2004. The size of the circle marking the location of each plant denotes the range of the plant's summer generating capacity in Megawatts (MW), as indicated by the key at the bottom left. Reprinted with permission from Platts, a division of McGraw-Hill Companies, Inc.

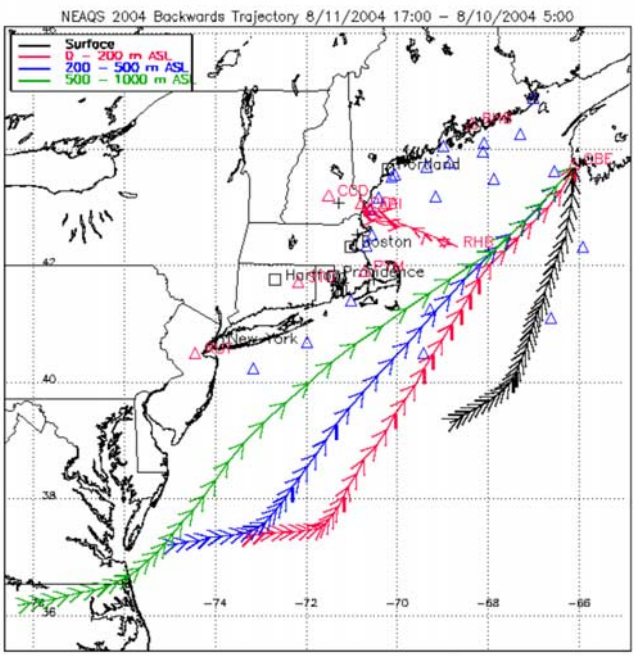

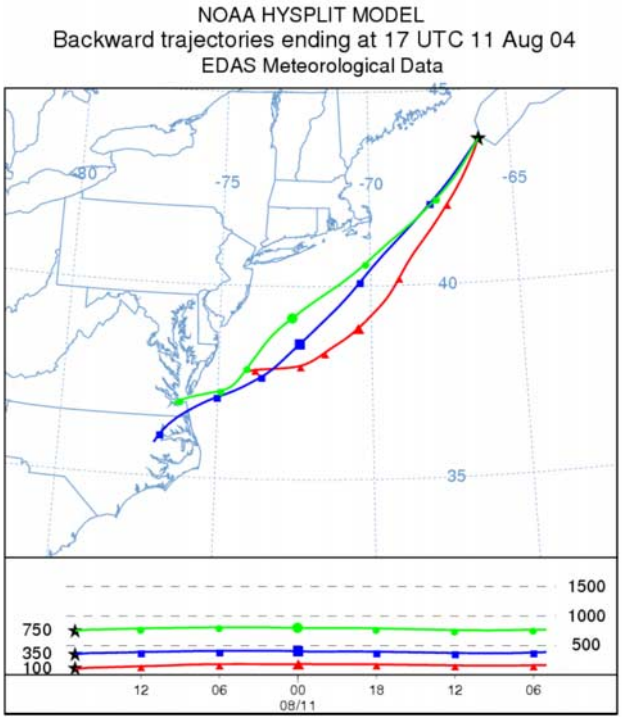

Figure 13. As in Figure 9 except ending at 1700 UTC on 11 August.

in real time, beginning in 2005, for the Texas Air Quality Study. The wind fields for this tool are derived primarily from networks of wind profilers that provide continuous, hourly, height-resolved observations of wind speed and direction. Over the Gulf of Maine and the Gulf of Mexico, surface trajectories can be computed using surface observations from NOAA and cooperative agency buoy and shoreline stations. The profiler trajectory tool complements the more sophisticated model trajectory tools that, for

example, can be run automatically on a regular basis for time receptor analysis or conceptual model development.

[25] The backbone of the nation's operational, all-weather, upper air wind observing system is still the rawinsonde, which provides wind profiles throughout the atmospheric column at 12-hour intervals. Unfortunately, the dense profiler networks that provide continuous hourly winds for documenting regional transport are generally only available in specialized research field campaigns, and there is still work that needs to be done to improve real-time instrument performance, especially with regard to removing interfering signals that lead to erroneous wind measurements (e.g., radio frequency interference, ground clutter, migrating birds). Once these problems are solved, it is our hope that the observing gap for atmospheric transport will be addressed in future upgrades to the nation's upper air observing system.

[26] **Acknowledgments.** We thank the dedicated engineering staffs in the Physical and Chemical Sciences Divisions of NOAA/ESRL for installing and maintaining the NOAA profilers used in this study. We thank the individual cooperative agency profiler operators and the Global Systems Division of NOAA/ESRL for providing cooperative agency profiler data. We thank Tom Shyka of the Gulf of Maine Ocean Observing System (GoMOOS) and the Physical Oceanography Group at the University of Maine for providing the GoMOOS and NOAA buoy and C-MAN station data used in the New England trajectory tool. The critical review provided by J. W. Bao and two anonymous reviewers helped improve the manuscript. The air quality study wind profiler deployments and related research were supported by the NOAA Health of the Atmosphere Program. We thank Susanne Hering and Nathan Kreisberg of Aerosol Dynamics for their work in developing and helping to deploy TAG. TAG measurements were supported by a U.S. Department of Energy SBIR Phase I and II grant (DE-FG02-02ER83825) and a graduate research fellowship for Brent Williams from DOE's Global Change Education Program.

References

Angevine, W. M. (1997), Errors in mean vertical velocities measured by boundary layer wind profilers, *J. Atmos. Oceanic Technol.*, *14*, 565–569.

Banta, R. M., et al. (1998), Daytime buildup and nighttime transport of urban ozone in the boundary layer during a stagnation episode, *J. Geophys. Res.*, *103*(D17), 22,519–22,544.

Banta, R. M., C. J. Senff, J. Nielsen-Gammon, L. S. Darby, T. B. Ryerson, R. J. Alvarez, S. P. Sandberg, E. J. Williams, and M. Trainer (2005), A bad air day in Houston, *Bull. Am. Meteorol. Soc.*, *86*(5), 657–669, doi:10.1175/BAMS-86-5-657.

Browning, K. A., and R. Wexler (1968), The determination of kinematic properties of a wind field using Doppler radar, *J. Appl. Meteorol.*, *7*, 105–113.

Carter, D. A., K. S. Gage, W. L. Ecklund, W. M. Angevine, P. E. Johnston, A. C. Riddle, J. Wilson, and C. R. Williams (1995), Developments in UHF lower tropospheric wind profiling at NOAA's Aeronomy Laboratory, *Radio Sci.*, *30*, 977–1001.

Chadwick, R. B. (1988), The Wind Profiler Demonstration Network paper presented at Symposium on Lower Tropospheric Profiling: Needs and Technologies, Am. Meteorol. Soc., Boulder, Colo., 31 May to 3 June.

Ecklund, W. L., D. A. Carter, and B. B. Balsley (1979), Continuous management of upper atmospheric winds and turbulence using a VHF Doppler radar: Preliminary results, *J. Atmos. Terr. Phys.*, *41*, 983–984.

Fehsenfeld, F. C., et al. (2006), International Consortium for Atmospheric Research on Transport and Transformation (ICARTT): North America to Europe: Overview of the 2004 summer field study, *J. Geophys. Res.*, doi:10.1029/2006JD007829, in press.

Fisher, E., A. Pszenny, W. Keene, J. Maben, A. Smith, J. Stutz, R. Talbot, C. Senff, and A. White (2006), Nitric acid phase partitioning and cycling in the New England coastal atmosphere, *J. Geophys. Res.*, *111*, D23S09, doi:10.1029/2006JD007328.

Frisch, A. S., B. L. Weber, R. G. Strauch, D. A. Merritt, and K. P. Moran (1986), The altitude coverage of the Colorado wind profilers at 50, 405, and 915 MHz, *J. Atmos. Oceanic Technol.*, *3*, 680–692.

Martner, B. E., D. B. Wuertz, B. B. Stankov, R. G. Strauch, E. R. Westwater, K. S. Gage, W. L. Ecklund, C. L. Martin, and W. F. Dabberdt (1993), An evaluation of wind profiler, RASS, and microwave radiometer performance, *Bull. Am. Meteorol. Soc.*, *74*, 599–613.

McNider, R., W. B. Norris, A. J. Song, R. L. Clymer, S. Gupta, R. M. Banta, R. J. Zamora, A. B. White, and M. Trainer (1998), Meteorological conditions during the 1995 SOS Nashville/Middle Tennessee field intensive, *J. Geophys. Res.*, *103*(D17), 22,225–22,243.

Meagher, J. F., E. B. Cowling, F. C. Fehsenfeld, and W. J. Parkhurst (1998), Ozone formation and transport in southeastern United States: Overview of the SOS Nashville/Middle Tennessee Ozone Study, *J. Geophys. Res.*, *103*(D17), 22,213–22,223.

Millet, D. B., et al. (2006), Chemical characteristics of North American surface layer outflow: Insights from Chebogue Point, Nova Scotia, *J. Geophys. Res.*, *111*, D23S53, doi:10.1029/2006JD007287.

Weber, B. L., D. B. Wuertz, D. C. Welsh, and R. McPeek (1993), Quality controls for profiler measurements of winds and RASS temperatures, *J. Atmos. Oceanic Technol.*, *10*, 452–464.

White, A. B., et al. (2006), Comparing the impact of meteorological variability on surface ozone during the NEAQS (2002) and ICARTT (2004) field campaigns, *J. Geophys. Res.*, doi:10.1029/2006JD007590, in press.

Wolfe, D. W., et al. (2006), Shipboard multi-sensor wind profiles from NEAQS 2004, *J. Geophys. Res.*, doi:10.1029/2006JD007344, in press.

Worthington, R. M. (2002), Comment on "Comparison of radar reflectivity and vertical velocity observed with a scannable C-band radar and two UHF profilers in the lower troposphere", *J. Atmos. Oceanic Technol.*, *20*, 1221–1223.

L. S. Darby and A. N. Keane, Earth System Research Laboratory, NOAA, Boulder, CO 80305, USA.

I. V. Djalalova, C. J. Senff, A. B. White, and D. E. White, Cooperative Institute for Research in Environmental Sciences, University of Colorado, Boulder, CO 80309, USA. (allen.b.white@noaa.gov)

A. H. Goldstein and B. J. Williams, Department of Environmental Science, Policy, and Management, University of California, Berkeley, CA 94720, USA.

D. C. Ruffieux, Aerological Station, MeteoSwiss, CH-1530 Payerne, Switzerland.